

Complex networks with tuneable dimensions as a universality playground

Ana P. Millán,¹ Giacomo Gori,² Federico Battiston,³ Tilman Enss,² and Nicolò Defenu^{4,2}

¹*Amsterdam UMC, Vrije Universiteit Amsterdam,*

Department of Clinical Neurophysiology and MEG Center,

Amsterdam Neuroscience, De Boelelaan 1117, Amsterdam, The Netherlands

²*Institut für Theoretische Physik, Universität Heidelberg, D-69120 Heidelberg, Germany*

³*Department of Network and Data Science, Central European University, 1051 Budapest, Hungary*

⁴*Institute for Theoretical Physics, ETH Zürich Wolfgang-Pauli-Str. 27, 8093 Zurich, Switzerland*

Universality is one of the key concepts in understanding critical phenomena. However, for interacting inhomogeneous systems described by complex networks a clear understanding of the relevant parameters for universality is still missing. Here we discuss the role of a fundamental network parameter, the spectral dimension, neglected in previous investigations. For this purpose, we construct a complex network model where the probability of a bond between two nodes is proportional to a power law of the nodes' distances. By explicit computation we prove that the spectral dimension for this model can be tuned continuously from 1 to infinity, and we discuss related network connectivity measures. We propose our model as a tool to probe universal behaviour on inhomogeneous structures and comment on the possibility that the universal behaviour of correlated models on such networks mimics the one of continuous field theories in fractional euclidean dimensions. We suggest that similar structures could be engineered in atomic, molecular and optical devices in order to tune universal properties to a desired value.

I. INTRODUCTION

Scale invariance is a key property of critical systems and leads to the appearance of power-law scaling in several macroscopic physical quantities close to the transition point. These power laws are often universal for a large variety of microscopically different systems [1], which only share the presence of a symmetry breaking transition and the specific symmetry of the order parameter. The existence of universality within the theory of critical phenomena was clarified several decades ago, thanks to the analogy between the thermodynamic limit of many body systems and the long-time behaviour of dynamical systems that was established by the renormalization group (RG) approach [2]. This success is exemplified by the study of phase transitions and spontaneous symmetry breaking in the paradigmatic $O(n)$ symmetric vector model [3]. The universal critical properties and scaling exponents depend only on the symmetry index n and on the euclidean spatial dimension d , which control the phase space for critical fluctuations. With recent extensions to fractional $d, n \in \mathbb{R}$, this model describes universal critical phenomena in a wide range of physical systems [4–6]. Going beyond the traditional case of thermal and quantum phase transitions [7, 8], applications of universality include cell membranes [9], turbulence [10], fracture and plasticity [11, 12] and epidemics [13].

Over the years, growing efforts have been devoted to map interacting systems and their complex patterns of connections into complex networks formed by a set of nodes and links describing their pairwise couplings [14]. Indeed, networks are able to provide a useful abstraction to characterize the architecture of many real systems, on top of which collective behaviour and criticality can emerge [15]. Comprehensive information on the structure of a network is provided by its *spectral dimension* d_s , which characterizes the scaling of the eigenvalues of the associated Laplacian matrix [16, 17]. In fact, the traditional RG description of critical phenomena, where scaling behaviour is influenced by diverging critical fluctuations, implicitly suggests the spectral dimension as the relevant control parameter for universal behaviour on inhomogeneous structures.

Long forgotten, this fundamental quantity has recently generated a new wave of interest [18–20] to characterize the structure of more complicated systems such as simplicial complexes, where couplings among constituents are not limited to pairwise interactions [21]. For many complex networks, the Fiedler (second smallest) eigenvalue remains finite in the thermodynamic limit, in which case the network is said to display a *spectral gap*. By contrast, if the spectral gap closes as the system size grows, the network is said to have a finite spectral dimension [17]. In parallel, geometrical investigations of network structures have sometimes considered the *Hausdorff dimension* (or fractal dimension) d_H , which characterizes the scaling of the number of neighbours of a node as a function of the network distance $N_n(\rho) \sim \rho^{d_H}$ [22, 23]. The Hausdorff dimension plays a key role in navigation and optimal transport problems [24–26].

The spectral dimension was found to be an important tool to understand dynamics on networks, which characterizes the return properties of the random walk [27] and the stability of the synchronised state [14, 28]. The role of the spectral dimension as a control parameter for universal behaviour in critical phenomena can be proven in quadratic models, such as the spherical model [29] and Dyson's hierarchical model [30, 31] in the mean field region. Its validity for correlated critical models has proven much harder to verify, despite several investigations on classical long-range systems [32–35], diluted models [36–38], spin glasses [39, 40] and quantum systems [34]. More

Over the years, growing efforts have been devoted to map interacting systems and their complex patterns of connections into complex networks formed by a set of nodes and links describing their pairwise couplings [14]. Indeed, networks are able to provide a useful abstraction to characterize the architecture of many real systems, on top of which collective behaviour and criticality can emerge [15]. Comprehensive information on the structure of a network is provided by its *spectral dimension*

over, several of these investigations rely on a conjectured relation between the universality of long-range interacting systems and that of local models with $d \in \mathbb{R}$, however this conjecture appears to hold only approximately [33, 41, 42].

Less explored, the role of the Hausdorff, or fractal, dimension in universal behaviour remains unclear. Seminal investigations of the Ising and percolation models show a nontrivial dependence of the scaling exponents on d_H close to zero temperature in fractals with $1 < d_H < 2$ [43–45]. Yet, the universal properties are found to depend also on other quantities, indicating a possible breakdown of universality in terms of d_H when $d_H < 2$ [43]. However, the fractal and spectral dimensions are related by the inequality $d_H \geq d_s \geq \frac{d_H}{d_H+1}$ [46, 47], and this opens up the exciting possibility of true universal scaling depending only on the spectral dimension at least on a restricted class of graphs, where non-trivial universal behaviour is observed.

In this work, we study a general complex network model with a tuneable spectral dimension in the range relevant for critical phenomena. This model is constructed in Sec. II from a one-dimensional nearest-neighbour chain, where additional long-distance bonds are inserted randomly with a probability that decays as a power law of the bond length. We compute the spectral dimension as a function of the power-law decay exponent σ and prove that it controls both the scaling of the spectrum (Sec. III) and the return times of *random walkers* (RWs) in Sec. IV. This provides a first demonstration of universal behaviour in this system. In Sec. V, we present our model as a platform to study universality and critical phenomena on complex networks. We define and compute the anomalous dimension of our complex network and find a striking resemblance to the anomalous dimension of the Ising universality class in fractional dimension. Finally, in Sec. VI we conclude with a discussion of the future perspectives of our findings.

II. MODEL

We consider a network of N nodes placed regularly on a circumference of radius 1, at locations $\theta_i = 2\pi i/N$, $i = 1, \dots, N$. The network is characterized by its adjacency matrix $A = \{a_{ij}\}$, where $a_{ij} \in \{0, 1\}$ indicates respectively the absence or presence of a link between nodes i and j . The coupling probability between any pair of nodes is given by

$$p_{ij} = \frac{1}{r_{ij}^{1+\sigma}}, \quad (1)$$

where $r_{ij} \neq 0$ is the distance between nodes i and j and σ is the model parameter characterising the scaling of the coupling probability with the (geometric) distance. Note that our network does not contain self loops, hence we only consider links with $i \neq j$. Consequently, the model

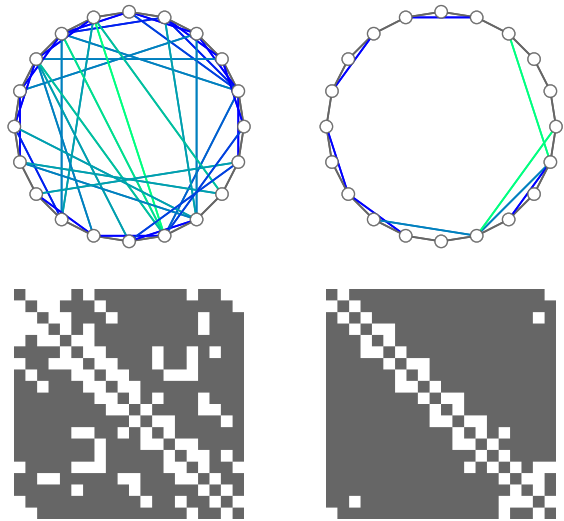


FIG. 1. Examples of the network layout for $N = 20$, $\sigma = 2/3, 3/2$ (left) and (right), respectively. The adjacency matrices are shown in the bottom row, indicating existing edges (white squares).

generates networks with tightly connected local neighbourhoods and increasingly rare long-range connections. As a robustness check for our results, we will consider two versions of the aforementioned model, based on different definitions of the distance

$$r_{ij}^{(L)} = \min(|i - j|, N - |i - j|), \quad (2)$$

$$r_{ij}^{(C)} = \sin\left(\frac{\pi}{N}|i - j|\right) / \sin\left(\frac{\pi}{N}\right), \quad (3)$$

for the linear (L) and circular (C) model.

Our network model can be considered as a one dimensional instance of the celebrated Kleinberg model [48], first introduced in two dimensions to investigate the emergence of the small-world phenomenon beyond the paradigm of Watts and Strogatz [49] and conventionally employed in the study of optimal transport problems [24–26]. Due to its connection with Kleinberg’s early proposal we denote our model K1d and, in the following, we show that its spectral properties are highly non-trivial and realise the whole range of spectral dimensions $d_s \in [1, \infty)$.

In the framework of critical phenomena, this model can be regarded as the giant cluster of a long-range percolation model well inside the percolating regime [35], so that the network always presents a nearest-neighbour connected ring backbone, $p_{i,i+1} = 1 \forall i$. Aside from network theory applications, the two-dimensional lattice version of this model has been already employed to investigate XY model dynamics [50, 51], epidemics spreading [52, 53] and critical behaviour on inhomogeneous structures [37, 38]. In contrast with the two-dimensional version, our one-dimensional model allows to realise low spectral dimension $d_s < 2$, which are expected to be very relevant in the study of universal behaviour for critical models with discrete symmetries, such as the Ising model

and percolation [43, 44]. An example of our network layout and adjacency matrices for two values of σ is shown in Fig. 1. For simplicity, we will here consider undirected symmetric networks with $a_{ij} = a_{ji}$.

The degree of each node measures its number of neighbours, $k_i = \sum_{j=1}^N a_{ij}$. In the infinite size limit $N \rightarrow \infty$, the degree distribution of the model is well approximated by a normal distribution as sketched in Fig. 2(a), see App. C for more details. The mean of the distribution is $\kappa = 2\zeta(\sigma + 1)$ and its standard deviation is $\sigma_\kappa = [2(\zeta(\sigma + 1) - \zeta(2\sigma + 2))]^{1/2}$, where $\zeta(s)$ is the Riemann Zeta function. Notice that in the $\sigma \rightarrow 0$ limit both κ and σ_κ diverge, as $\lim_{s \rightarrow 1} \zeta(s) = +\infty$. In the opposite limit $\sigma \rightarrow \infty$, the network converges to a ring chain with $\kappa = 2$ and $\sigma_\kappa = 0$.

Many real-world networks are characterised by the presence of efficient pathways of communications. They can be quantified by the average path length ℓ , which measures the mean topological distance between every pair of nodes over the network shortest paths:

$$\ell = \frac{1}{N(N-1)} \sum_{i=1}^N \sum_{j \neq i} \rho_{ij}, \quad (4)$$

where ρ_{ij} is the minimum number of links connecting nodes i and j , i.e. the topological distance. The cumulative distribution of ρ_{ij} , $P(\rho)$, indicates the average fraction of nodes that are within a radius ρ of any given node. This is shown in Fig. 2(b) for different values of σ ; it indicates how for small σ the fraction of neighbours grows quickly with the distance ρ , whereas for $\sigma \gg 1$ the nodes' neighbourhoods scale as a power-law of the distance – the exponent of which gives the Hausdorff dimension (see App. D).

In general, low values of ℓ relative to the network size indicate the emergence of the small-world phenomenon [49], associated to an efficient behaviour of a communication network [54]. More formally, a network is said to display such a property if ℓ grows proportionally to the logarithm of its nodes [55], a feature of multiple graph models including Erdős-Rényi networks [56].

An empirical property of many real-world networks is the presence of dense local structures, which can be for instance quantified by means of the network transitivity T , defined as

$$T = \frac{\text{number of closed triangles}}{\text{number of open triads}}, \quad (5)$$

This feature is absent in Erdős-Rényi and similar random graph models, but present in the K1d model.

Similarly to the original Watts-Strogatz model [57], the K1d model is characterised by a regime of intermediate values of σ which maximizes transitivity whereas displaying efficient communication structure, as shown in Fig. 2(c). The analysis pursued in Ref. [58] already showed that the connectivity properties of this kind of models change their nature as a function of σ . The $\sigma > 1$

case shall not possess small world properties, while displaying high clustering features. When the probability of long-distance connections grows for $\sigma < 1$, the topology of the network changes and the topological distance seems to display sub-power law scaling still maintaining finite clustering. The sub-power law scaling of the topological distance in the thermodynamic limit can be proven exactly, see Ref. [59]. Finally, for $\sigma < 0$ the network actually becomes small-world and the clustering vanishes in the thermodynamic limit. The transitions between these different topological regimes appear to be continuous similarly to conventional second order phase transitions.

In the following we are going to show how these “continuous transition’s” also influences the spectral properties of the network, even if the evolution of the spectrum appears to be far more involved than the one of the topological properties.

III. SPECTRAL PROPERTIES

In order to evaluate the spectral dimension d_s of the K1d model, we consider the graph Laplacian \mathcal{L} [60]

$$\mathcal{L}_{ij} = \begin{cases} 1 & \text{when } i = j \\ -\sqrt{\frac{1}{k_i k_j}} & \text{if } a_{ij} = 1 \\ 0 & \text{otherwise} \end{cases}. \quad (6)$$

and numerically evaluate its spectrum as a function of σ for several realisations of the K1d model. The convergence properties of the spectrum have been studied by calculating it for increasing network sizes up to $N = 2^{12}$. The numerical estimates for the spectrum upon increasing the number of network realisations or the network size have been shown to converge to the same function, indicating self-averaging properties and yielding a unique definition of spectral dimension d_s in the thermodynamic limit. The numerical spectra of the K1d model with linear distance definition (K1d^(L)) have been compared with the ones obtained with the circular distance definition (K1d^(C)), proving the isospectral property of the two models in the thermodynamic limit $N \rightarrow \infty$.

The eigenvalues of the normalized Laplacian have been ordered based on their magnitude and are denoted by ω_i , with $\omega_1 = 0$ being the eigenvalue of the steady-state eigenvector. The ordered spectra are shown in Fig. 3 for $\sigma = 0.0, 0.5, 1.5$ for various network sizes L . In all cases the spectra converge to a well defined functional form at large N , but finite size corrections are more relevant for smaller σ . As expected, both the $\sigma > 0$ cases present a continuous power law behaviour at $\omega_i \simeq 0$, indicating a low energy DOS for vibrational modes of the form

$$\mathcal{D}(\omega) \propto \omega^{d_s-1} \quad (7)$$

with a finite value of the spectral dimension d_s . For $\sigma = 0$ the spectrum appears to develop a finite gap $\omega_2 - \omega_1 \neq$

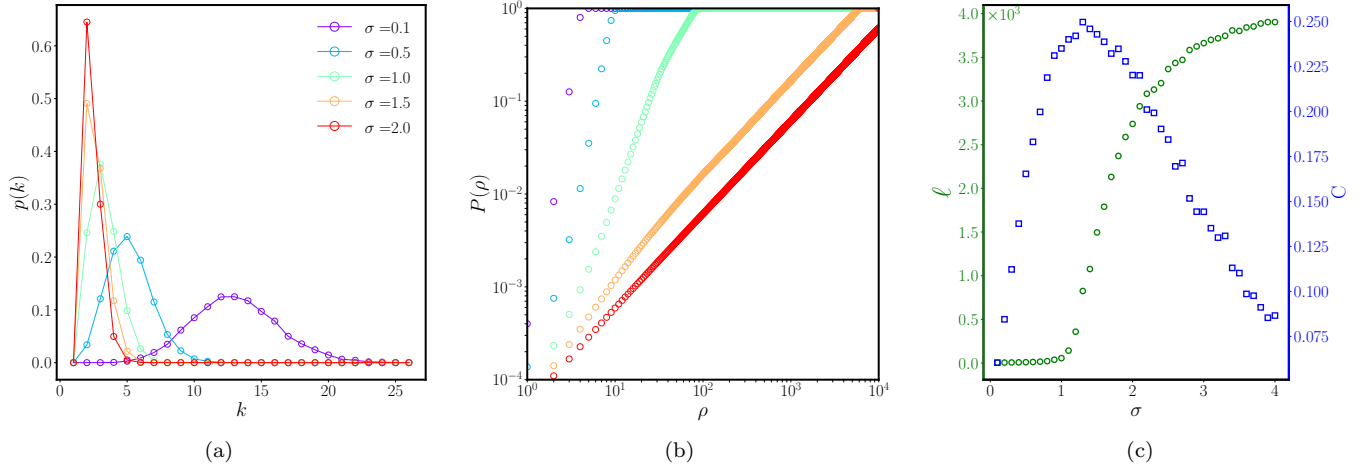


FIG. 2. Network statistics as function of σ for $N = 2^{16}$ for the symmetric model with linear distance definition $\text{K1d}^{(L)}$. (a) Degree distribution $p(k, \sigma)$ for five representative values of $\sigma = \{0.1, 0.5, 1.0, 1.5, 2.0\}$ from bottom to top, see legend. (b) Average fraction of nodes at a given topological distance ρ , $P(\rho, \sigma)$, for the same values of σ . (c) Mean minimum path $\ell(\sigma)$ (green points, left y-axis) and transitivity $C(\sigma)$ (blue squares, right y-axis).

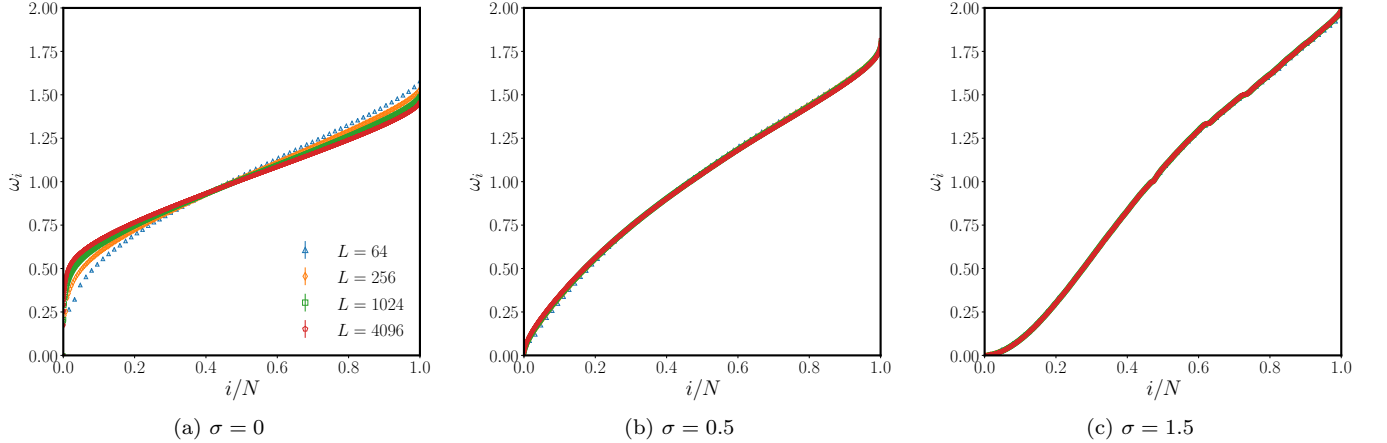


FIG. 3. Spectra (averaged over different realisations) for (a) $\sigma = 0$ (b) $\sigma = 0.5$ and (c) $\sigma = 1.5$ for increasing system size. All three spectra refer to the linear model.

0 indicating that $d_s = \infty$. According to this analysis the point $\sigma = 0$ does not only delimit the topological transition from a non small-world network $\sigma > 0$ to a small-world one at $\sigma < 0$, but also the appearance of a spectral gap in the model, which persists for all $\sigma < 0$.

In order to justify these observations on theoretical grounds one may construct the following analytically solvable model, which shares several features with the K1d. We consider the average over all possible realisations of the adjacency matrix of our model $\bar{a}_{ij} = p_{ij} = 1/r_{ij}^{1+\sigma}$, which describes a fully connected weighted graph. The lack of translational invariance in the K1d model is removed by the averaging procedure and the spectral dimension of the resulting graph is analytically

known as

$$d_s = \begin{cases} 2/\sigma & \text{if } 0 < \sigma < 2 \\ 1 & \text{if } \sigma \geq 2, \end{cases} \quad (8)$$

see Ref. [61]. In principle, we do not expect the estimate in Eq. (8) to exactly reproduce the spectral dimension of the K1d model, since taking the average directly on the adjacency matrix is not the same as taking it on the spectrum¹. However, based on the analogy with the problem of long-range percolation one may expect this

¹ Note that this procedure would correspond to take the *annealed* version of the model in the language of disordered systems. Our study will be rather devoted to the *quenched* case.

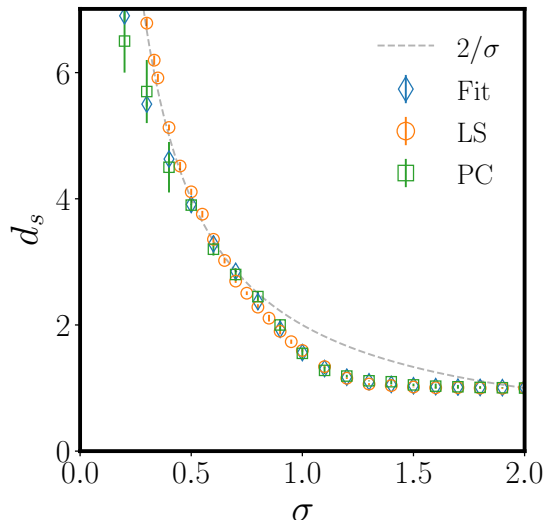


FIG. 4. The spectral dimension d_s of the model obtained by the finite size scaling of the Laplacian spectrum (LS), orange circles, by the power law return probability of the random walk (Fit), blue diamonds and by the collapse of the return probability (PC), green squares. The dashed grey line represents the analytical expectation in Eq. (8).

result to be accurate both at $\sigma > 2$, where the effect of long-range connectivity becomes irrelevant to the universal behaviour, and at $\sigma < 1/3$, where the universal behaviour of the percolation model lies in the mean-field regime.

A direct fit to the low-energy tails of the spectra in Fig. 3 does not yield reliable estimates for the spectral dimension values. Then, we shall rely on finite size scaling properties. Indeed, in order for the spectrum to display the expected power law behaviour in the thermodynamic limit, each finite size eigenvalue should exhibit the leading order scaling

$$\omega_i^{(N)} \propto N^{-2/d_s}. \quad (9)$$

Using Eq. (9) we can extract the spectral dimension from the finite size scaling of the low lying eigenvalues, see App. A. The resulting values for the spectral dimension as a function of σ are reported as orange circles in Fig. 4.

IV. RANDOM WALK

A. Return probability

A first indication of the role of the spectral dimension as a control parameter for universal behaviour is found in its appearance in the scaling behaviour of random walkers after a large number of steps. In particular the return probability of a random walker to the origin after t steps

on an inhomogeneous structures shall obey [16, 17, 62]:

$$P_0(t) \sim t^{-d_s/2}, \quad t \gg 1. \quad (10)$$

In order to prove that such a universal relation is obeyed in our model, we numerically computed the return probability $P_0(t)$ on different realisations of our network. Initially the walker is placed on a random node i , and at each time step it jumps with uniform probability $1/k_i$ to a neighbouring node. The walker is left to diffuse for a number of steps τ large enough to explore a macroscopic portion of the network. The results for the return probability shown in the paper have been obtained by averaging over $N_R = 10^5$ random walk's trajectories on each network realisation with $\tau = 10^5, 10^6$.

The value of d_s as a function of σ has been estimated using a maximum likelihood algorithm [63, 64]. For each value of the network size N and of the decay exponent σ this technique requires the identification of an initial time t_{min} and a final time t_{max} , between which one has to pursue the power-law fit. Indeed, the scaling behaviour cannot appear at small times, as the return probability in this limit is highly influenced by the local structure of the K1d model and by the absence of self-links, such that $P_0(2t - 1) < P_0(2t)$ and then Eq. (10) shall not be obeyed at small t . On the other end, finite size effects still appear at very large times, particularly for small σ as, due to the high connectivity, the random walkers can loop over the network faster in this case. The observation of more prominent finite size effects at small σ is consistent with the behaviour observed in Fig. 3 for the Laplacian spectrum.

Therefore, the scaling behaviour of Eq. (10) can only be observed for intermediate values of times and very large network sizes, leading to the necessity of identifying a proper time window to estimate the power law decay exponent. In order to proceed with the d_s estimations in this case, we select an initial sensible value of t_{max} for each N and σ pair and then optimise both the time boundaries t_{min} and t_{max} making use of a maximum likelihood algorithm adapted from Ref. [65]. Note that for small σ ($\sigma < 0.5$) the finite size effects can appear before t_{min} , leading to the underestimation of d_s . Consequently, very large systems are necessary to estimate d_s in this case, blue diamonds in Fig. 4.

B. Finite size effects on d_s

Given the picture above, it is evident that finite size corrections are expected to hinder the accuracy of the d_s estimations from the random walk return probabilities, especially in the $\sigma \rightarrow 0$ limit where such corrections appear already at short times even for large sizes. In order to overcome these difficulties, we exploited the universal nature of the return probability and introduced the finite size scaling of $P_0(t)$ as

$$P_0^N(t) = \frac{1}{N} f\left(Nt^{-d_s/2}\right), \quad (11)$$

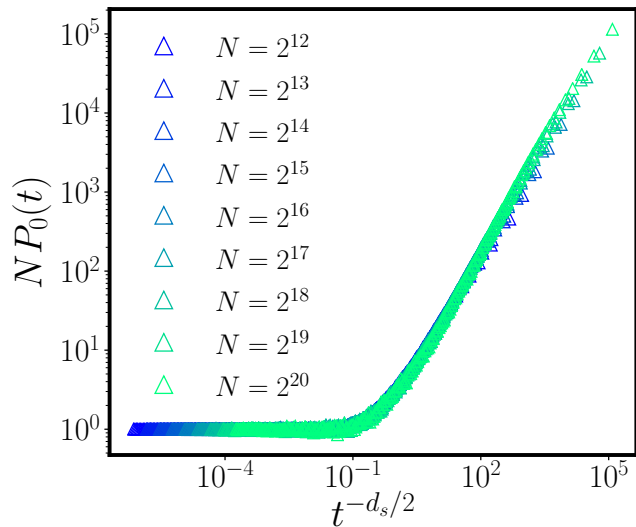


FIG. 5. Collapse of $P_0(t)$ for $\sigma = 0.5$ and $N = 2^i$, $i = 12, 13, \dots, 20$ using the scaling function in Eq. (11).

with $f(x)$ such that $f(x) \propto x$ for $x \gg 1$ and $f(x) \propto O(1)$ for $x \ll 1$. The latter finite size scaling ansatz can be used to scale the return probabilities curves of different network sizes $P_0^N(t)$ on each other, thus yielding an estimate of d_s by the optimal value for the collapse. This procedure is exemplified in Fig. 5 for $\sigma = 0.5$; the optimal value for d_s found in this case is $d_s \simeq 3.91$.

The spectral dimension results from the probability collapse (PC) are shown as green squares in Fig. 4. Finite size effects also affect the collapse results for the spectral dimension d_s at $\sigma \lesssim 0.5$, but the errorbars estimates are more reliable with this method, when compared to the simple large time fit. In general, the comparison between random walk estimates, both by power law fits (Fit) and by the return probability collapse (PC), yield consistent estimates in the whole σ range and almost perfectly reproduce the laplacian spectrum (LS) results for $\sigma \gtrsim 1/2$ corresponding to $d_s \lesssim 4$. The agreement between the different approaches not only furnishes a precise estimate of the spectral dimension in the most relevant range for critical $O(n)$ models, which exhibit trivial mean-field criticality for $d \equiv d_s > 4$, but also proves the universality of the random walk dynamics and, then, provides a first hint on the universal role of the spectral dimension on these networks [17, 66].

V. A UNIVERSALITY PLAYGROUND

A. Previous results

The current understanding of critical phenomena is rooted in the study of prototypical models, which—in spite of their simplicity—can produce accurate predictions for real physical systems thanks to the universality

phenomenon. Following this path, for most of the experimentally observed critical behaviour it has been possible to construct a continuous field theory model, which reproduces the appropriate universal quantities without any information about the discrete nature of the microscopic variables and the lattice structure. A paradigmatic example of this procedure can be found in the characterisation of the universality of homogenous spontaneous symmetry breaking via the $O(n)$ symmetric models. These models describe a vector order parameter φ with n components, whose ground state value may be either $O(n)$ symmetric $|\varphi_0| = 0$ or spontaneously symmetry broken $|\varphi_0| \neq 0$.

The early picture for the universal behaviour of $O(n)$ models was first obtained by perturbative RG [67–70] and has since then been complemented with several real-space and variational results [71–73]. More recently, functional RG approaches [74–76] have been able to reproduce and extend previous findings, yielding the full universal landscape for $O(n)$ field theories [5, 6, 77–81]. With these extensive investigations, $O(n)$ models have become the general tool for the understanding of universal behaviour in critical phenomena.

In these systems the only relevant parameters regulating universal behaviour are the symmetry index n and the euclidean spatial dimension d : they control the phase space for critical fluctuations by altering, respectively, the number of fluctuating modes and the low-energy tails of the density of states (DOS). Interestingly, the universal properties can be analytically continued to the two-dimensional plane $(d, n) \in \mathbb{R}^2$, leading to a complex phase diagram which has been a fundamental ingredient in the understanding of universality [82–87].

The intricacies regarding the proper definition of dimension on graphs have, up to now, hindered the validation of the existing theoretical results for universal behaviour in fractional dimension on discrete inhomogeneous structures. Yet, theoretical investigations alone have reached a fair degree of consistency and unity among each other, yielding a comprehensive picture of the critical exponents of $O(n)$ models in the continuum with euclidean dimension $2 \leq d \leq 4$ [3, 5, 6, 72, 73]. For integer euclidean dimensions $d \in \mathbb{N}$, this picture can be verified by numerically exact results obtained by MC simulations [3], and, at least for the Ising model ($n = 1$), conformal bootstrap results, which are believed to be exact and also extend to $d \in \mathbb{R}$ [88], see Fig. 6.

The results depicted in Fig. 6 prove the capability of current theoretical approaches to provide reliable estimations of universal quantities in $O(n)$ field theories. Yet, no numerical confirmation or exact proof of the applicability of these results to microscopic discrete models exists. As anticipated above, the natural candidate for the dimension—as a relevant parameter for universality—on graphs and complex networks is the *spectral dimension* [17, 92, 93]. Indeed, the existence of the critical point for $O(n)$ symmetric models on complex networks is solely determined by the value of the spectral dimension,

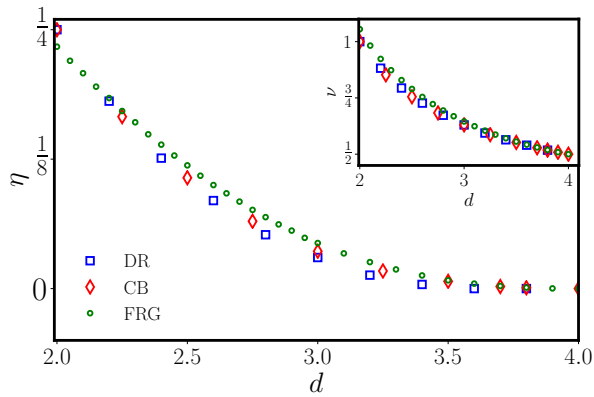


FIG. 6. Critical exponents of the Ising model as a function of $d \in [2, 4]$ from dimensional regularization (DR) [89], conformal bootstrap (CB) [4, 90, 91] and functional renormalization group (FRG) [5, 6].

at least as long as $d_s > 2$ [93–96]. Finally, the universal properties of most exactly solvable models, including the $O(n)$ models in the $n \rightarrow \infty$ limit, only depend on d_s [97–100].

The numerical confirmation of the above picture in correlated critical models is lacking, even in the simpler case of continuous symmetry $n \geq 2$ where no universal behaviour is found at $d_s \leq 2$. This is mostly due to the difficulty of identifying proper graph models that present both a tuneable spectral dimension and a stable numerical behaviour in the limit of large size. Indeed, mathematically exact derivations of the spectral dimensions of fractals are known only in few cases, usually with $d_s < 2$ [101–103], while numerical simulations need large sample sizes and long computation times [104]. It is worth noting that the few already existing examples of graphs with tuneable d_s are pathological and present neither anomalous random walk diffusion [105] nor correlated critical behavior [66]. Therefore, they do not provide good candidates for the realisation of universal behaviour in fractional dimension.

B. Universality of the spectral properties

In order to relate our studies to the aforementioned picture of universality, it is useful to consider our findings in the perspective of the long-range percolation problem discussed in Ref. [35]. In this problem each possible link of a one-dimensional chain is present with probability $p_{ij} = p r_{ij}^{-(d+\sigma)}$. This leads to the existence of a percolation threshold p_c at which critical scaling appears. Then, the complex network model introduced in Sec. II can be regarded as the giant cluster of the long-range percolation problem well inside the percolating regime with $p = 1 \geq p_c \forall \sigma$.

From this point of view, the problem of *long-range* percolation on a one-dimensional ring may be regarded as

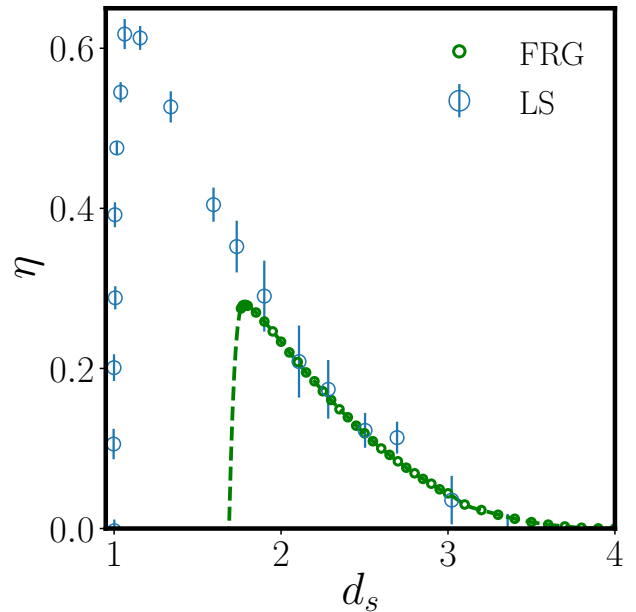


FIG. 7. The anomalous dimension generated by long-range disorder, as defined by Eq. (12), is compared to the FRG estimates of the anomalous dimension of the Ising model as a function of the Euclidean dimension d . The dashed curve represents a numerical extrapolation of the FRG data.

an instance of *nearest-neighbour* percolation on the complex graph analysed in the present paper. In Ref. [35] the critical properties of the long-range problem have been related to those of nearest-neighbour percolation in an effective fractional dimension $d_{\text{eff}} = \frac{(2-\eta_{\text{sr}})d}{\sigma}$, where η_{sr} is the anomalous dimension of the nearest-neighbour problem in dimension d_{eff} , as usual in the long-range literature [32–35]. The contribution of the anomalous dimension to the effective dimension is necessary to take into account the renormalisation of the field scaling dimension as compared to the case of quadratic models.

Therefore, in analogy with the case of long-range critical phenomena, one may interpret the deviation between the spectral dimension of the K1d model and the annealed estimate (8) as an *anomalous dimension* η due long-range disorder according to the formula

$$d_s = \frac{2 - \eta}{\sigma}. \quad (12)$$

In Fig. 7, the values of η obtained via Eq. (12) are reported and compared with those of the Ising model obtained by FRG, which also yields non-vanishing results for $d < 2$, specifically down to $d \approx 1.76$. The similarity between the two curves is not surprising as the anomalous dimensions of several correlated models have similar trends [5, 6].

The η curve in Ref. 7 furnishes further evidence of the connection between universal properties on network structures as function of d_s and the universality of corre-

lated models in Euclidean fractional dimension d . Note that the quantity η defined by Eq. (12) is not, strictly speaking, a critical property and we only refer to it as universal as it should not depend of the value of p as long as $p > p_c$. Indeed, an exact relation between the spectral properties of the percolating cluster and the critical exponents of the long-range percolation transition should only exist at $p = p_c$, however at this point the spectral dimension should be nearly constant [106, 107].

VI. CONCLUSIONS

From the human brain [108] to particles and grains [109], networks are the natural tool for a formal description of systems made up of many interacting agents. Over the years, a wide variety of dynamical processes have been studied on networks, from epidemic spreading [110] and diffusion [27] to synchronisation [28]. While it is well known that the exact form of interactions can affect the emergent dynamics [14], the link between network structure and critical behavior [111] is still far from understood.

Going beyond the individual assessment of specific network features, including average path length, clustering coefficient [57] or the heterogeneity of the degree distribution [112], in this paper we turned our attention to more fundamental network dimensions, such as the spectral and the Hausdorff dimensions, which govern universality in interacting systems. To this end, we have introduced a complex network model based on the one-dimensional percolation problem studied in Ref. [35]. This model, which we name K1d, coincides with a one-dimensional generalisation of the Kleinberg model [48].

Using extensive numerical simulation, we have characterized the spectral dimension d_s , which appears both in the scaling of the Laplacian spectrum and in the random walk return rates, and proved that it can be continuously tuned in the interval $d_s \in [1, \infty)$. Taken together, our model offers a valuable tool to study dynamical phenomena in presence of a complex, but now well characterised, spectral landscape, offering insights into fundamental aspects of universal and critical behaviour arising from network dynamics.

The importance of these investigations goes far beyond the mere curiosity towards the validity of field theory results in non-integer dimensions and relates to fundamental applications in several fields of contemporary physics, such as quantum technology and network science. In general, quantum technological applications, and in particular quantum simulation, demand efficient protocols for quantum state preparation, which may be attained by adiabatic protocols [113, 114]. In such schemes, internal system parameters are initially tuned to admit a ground state with very low entropy. Then, they are changed slowly until the target Hamiltonian is realized [115]. However, adiabaticity cannot be achieved in finite time when crossing a critical point, and a finite

defect density always arises at finite ramp speed [116].

The emergence of such finite corrections is governed by a universal power-law scaling, which usually only depends on the equilibrium critical exponents according to the celebrated Kibble-Zurek mechanism [117, 118]. Therefore, quantum state preparation often encounters universal bounds [119] that are influenced by the spectral dimension, as is the case in long-range interacting systems [120, 121]. In this perspective, the tuneability of universal exponents on specific complex networks, together with the possibility to realise such structures in trapped ion [122] and Rydberg atom [123] quantum simulators, provide candidates to devise new experimental systems that are more efficient for adiabatic state preparation.

Meanwhile, the network community has recently seen a surge of interest in the spectral dimension to connect the topological and geometrical properties of a network [124, 125] with its dynamics. So far, these explorations have mostly focused on systems interacting beyond traditional pairwise mechanisms [21]. In particular, the study of the spectral dimension of certain simplicial complexes [126, 127] via a renormalization group approach has yielded accurate relations between d_s and the topological dimension of the model [18]. Moreover, the spectral dimension was shown to be crucial to determine the synchronisation properties of the simplicial implementation of the Kuramoto model recently suggested in [128], and to affect diffusion properties at long time scales [19, 129]. These works could only consider a finite number of d_s values very close to the topological dimension of the building blocks of their network and they do not offer any realisation of tuneable $d_s > 2$ values. We are convinced that the introduction of a model with continuously tuneable spectral dimension such as the K1d model will pave the way to further investigations of the role of topology in network dynamics.

Acknowledgements: The authors acknowledge fruitful discussions with Fabiana Cescatti, Miguel Ibáñez-Berganza and Andrea Trombettoni during various stages of this work. This work is supported by the Deutsche Forschungsgemeinschaft (DFG, German Research Foundation) via Collaborative Research Centre “SFB1225” (ISOQUANT) and under Germanys Excellence Strategy “EXC-2181/1-390900948” (the Heidelberg STRUCTURES Excellence Cluster). F.B. acknowledges partial support from the ERC Synergy Grant 810115 (DYNASNET). A.P.M. also acknowledges support from the “European Cooperation in Science & Technology” (COST action CA15109) and from ZonMw and the Dutch Epilepsy Foundation, project number 95105006.

Appendix A: Low lying spectrum

We detail here the structure of the low lying spectrum as obtained by exact diagonalisation of the graph Laplacian (6). In Fig. 8 the first ten nonzero eigenvalues are

depicted as a function of the system size (averaged over 128 realisations) for sizes up to $N = 2^{13}$ for two different values of σ . As one can notice the power law decay is clearly attained for larger systems for all the depicted eigenvalues but the first eigenvalues display some oscillations that become smaller for the higher eigenvalues. Moreover, especially for small σ the eigenvalues tend to organise into doublets, thus estimation of d_s from a single eigenvalue could be affected by over/undershoot. In order to minimise the above effects we obtained our best estimates from the average of ω_{10} and ω_{11} fitted with a power law $\propto N^{-2/d_s}$, for sufficiently big sizes $N \geq 2^{10}$. The resulting estimations for the linear and circular models were mutually compatible supporting our estimation. Numerical work was not restricted to linear and circular model but we also considered: graphs with a thicker backbone (with next to nearest and next to next to nearest neighbours always turned on), models with non-backbone probabilities halved ($p_{ij} \rightarrow p_{ij}/2$) and doubled ($p_{ij} \rightarrow 2p_{ij}$). All of these models, albeit possessing a different spectrum reflecting the different nonuniversal features, share the same low lying spectrum behavior lending support to the universality of d_s for models with the same decay exponent σ .

Appendix B: Computational method to estimate d_s from $P_0(t)$

An illustration of the method used to measure d_s , as indicated in the main text, is shown for two different values of σ in Fig. 9. First, $P_0(t)$ is represented in a log-log scale, and a power-law function via a maximum likelihood algorithm [65] that finds optimal values of t_{min} and t_{max} . In case of a pronounced finite size effect, as in Fig. 9(b), an initial t_{max} is considered to avoid fitting of the flat part of $P_0(t)$.

Appendix C: Characterisation of K1d networks

In the infinite size limit ($N \rightarrow \infty$), the mean degree of the directed K1d networks, without imposing network symmetry, is given by

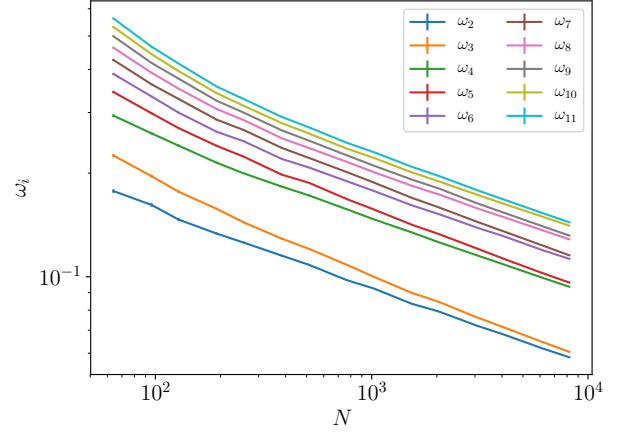
$$\kappa^D = 2\zeta(\sigma + 1), \quad (C1)$$

whereas the standard deviation of the degrees is

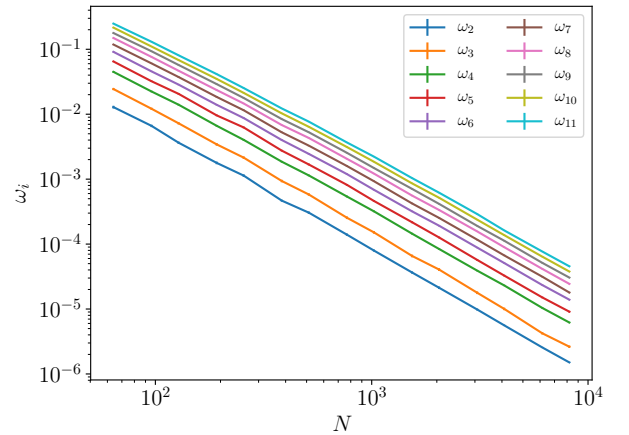
$$\sigma_\kappa^D = [2(\zeta(\sigma + 1) - \zeta(2\sigma + 2))]^{1/2}. \quad (C2)$$

In our random walkers analysis, the networks are made symmetric by defining $a_{ij}^S = \max(a_{ij}, a_{ji})$, that is, an undirected link is placed between nodes i and j when at least one directed edge is present. In this condition the mean degree and its standard deviation are given by:

$$\kappa = 2\zeta(\sigma + 1) - \zeta(2\sigma + 2), \quad (C3)$$



(a) $\sigma = 0.5$



(b) $\sigma = 1.3$

FIG. 8. First ten eigenvalues for (a) $\sigma = 0.5$ and (b) $\sigma = 1.3$ for sizes up to $N = 2^{13}$ in the circular model.

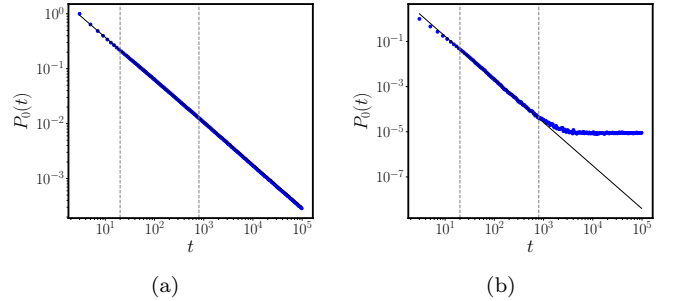


FIG. 9. Example of d_s fit. $P_0(t)$ is fitted in the region between the dashed lines. In panel (a), $\sigma = 1$, and finite size effects are not strong in this range of t . Estimated value: $d_s = 1.569 \pm 0.004$. In panel (b), on the contrary, $\sigma = 0.5$ and finite size effects appear early on. Estimated $d_s = 3.79 \pm 0.03$.

$$\sigma_\kappa = [2(2\zeta(\sigma+1) - 5\zeta(2\sigma+2) + 4\zeta(3\sigma+3) - \zeta(4\sigma+4))]^{1/2}. \quad (\text{C4})$$

This theoretical curves are shown in panel A of Fig. 10 together with the respective numerical estimates. These differences between the topological properties of the undirected and symmetrised directed K1d networks do not influence the low energy spectrum and, thus, do not alter the spectral dimension results.

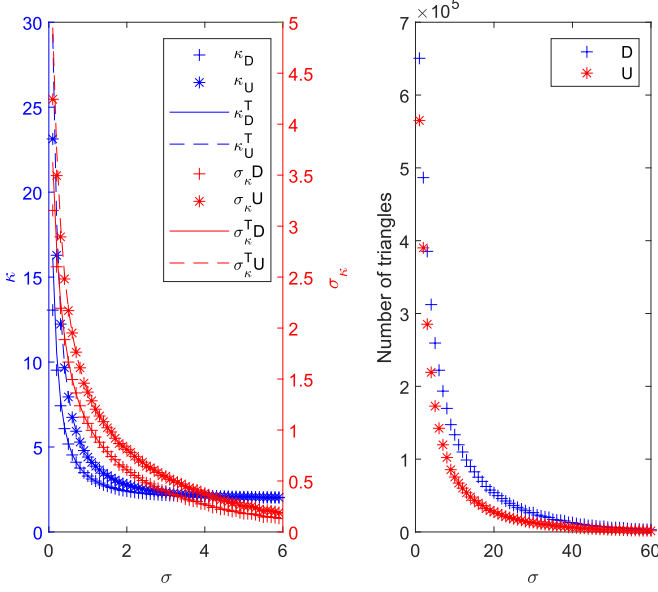


FIG. 10. (a) Dependence of the mean degree κ (left y-axis) and its standard deviation σ_κ (right y-axis) on σ , both for the directed and undirected cases. (b) Number of triangles in K1d as a function of σ , both for the directed and undirected cases.

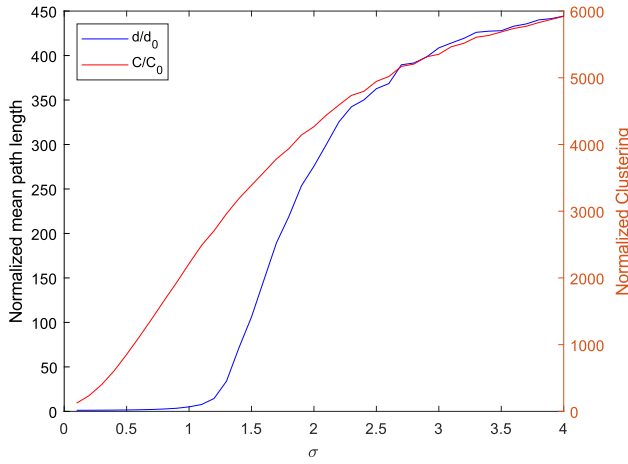


FIG. 11. Normalized mean path length $\ell(\sigma)/\ell_0(\sigma)$ and clustering coefficient $C(\sigma)/C_0(\sigma)$ of the model. Null model: Theoretical expectation for ER network with equal N and L as the corresponding K1d network.

In panel b of Fig. 10 we show the number of triangles presents in the network (N_T) as a function of σ , from which the clustering coefficient is calculated [55, 57]. As it can be seen, the number of triangles diverges as $\sigma \rightarrow 0$ and vanishes as $\sigma \rightarrow \infty$, where the network becomes a 1D circular chain. Moreover, in the $\sigma \rightarrow 0$ limit, the total number of possible triangles (given by κ), diverges faster than N_T , and therefore the clustering remains small, as shown in the main text. In Fig. 11 we show the clustering coefficient and mean path length of K1d networks normalised over the corresponding values of the null model given by random Erdős-Rényi (ER) networks with the same size (N) and number of edges ($L = N\kappa$). As can be seen, K1d networks always have higher clustering and average distance than equivalent ER networks. As $\sigma \rightarrow 0$, K1d become increasingly random and the difference decreases.

Appendix D: Hausdorff dimension and *small-world* nature of K1d networks

While compelling evidence exists to support the role of the spectral dimension as a control parameter for universal properties in critical models with continuous symmetry [93–95], the situation appears to be more complicated in discrete symmetric ones such as Ising and percolation models [43, 44, 106, 130–132]. This may be due to the

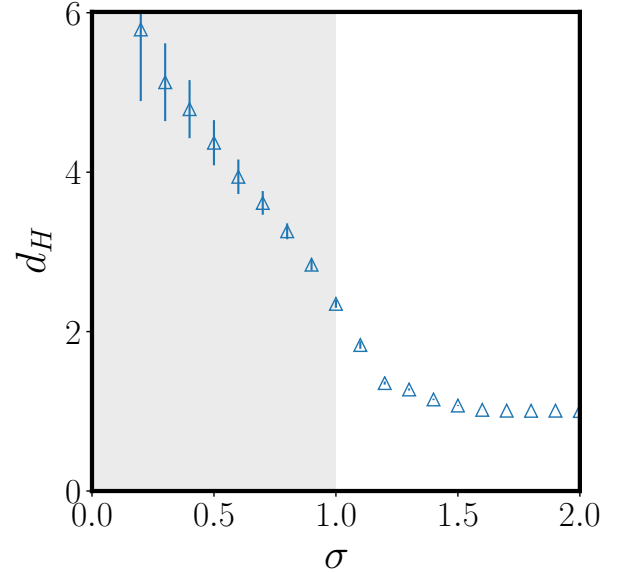


FIG. 12. The “effective” Hausdorff dimension of the $K1d^{(L)}$ model as a function of σ , determined by assuming a power law scaling of the number of neighbours of each node, see Eq. (D1). For smaller decay exponents $\sigma \lesssim 0.5$ the Hausdorff dimension results also become less accurate due to increasing finite size corrections. However, it is worth noting that contrary to the spectral dimension case the Hausdorff dimension values are only significant for $\sigma > 1.0$.

differences appearing in the large size scaling of regular lattices and complex networks. Indeed, while on regular lattices the Euclidean dimension regulates both the spectral properties and the scaling of the number of neighbours at large distances ($d_s = d_H = d$), this is not a general property of inhomogeneous graphs. In general, the scaling of the number of neighbours of a node with the distance, $N_r(\rho)$ (see Fig. 2(b)), is characterised by the Hausdorff dimension d_H :

$$N_r(\rho) \sim \rho^{d_H}, \quad (\text{D1})$$

if such a scaling can be found. In this case, d_H also describes the scaling of the network average distance, as indicated by its average path length ℓ , with its size: $\ell \sim N^{d_H}$. Networks with the *small-world* property have neighbourhoods quickly covering the whole network, that is, N_r grows exponentially with ρ , formally corresponding to $d_H \rightarrow \infty$. Conversely, distances in these networks grow as $\ell \sim \log(N)$.

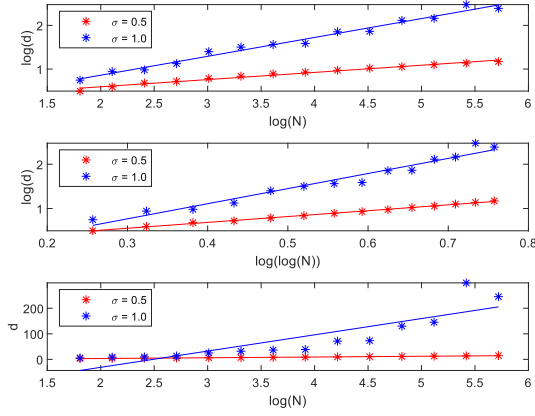


FIG. 13. Example of $\ell(N)$ fits for $\sigma = 0.5$ and $\sigma = 1.0$. Top panel: power-law fit $\ell(N) \sim N^{1/d_H}$. Mid panel: mixed fit $\ell(N) \sim \log(N)^\alpha$. Bottom panel: small-world fit $\ell(N) \sim \log(N)$.

The Hausdorff and the spectral dimension are related according to [46, 47]: $d_H \geq d_S \geq \frac{d_H}{d_H+1}$, with the euclidean lattices corresponding to the limiting case $d_H = d_s = d$. Consequently, there can be small-world networks with finite spectral dimension. In this case, the debate over the role each dimension plays on the dynamics is still open and, our model, may also provide an important tool to investigate these questions.

Previous studies on the Kleinberg model [58] indicate that, in dimension $d = 1$, the Hausdorff dimension is finite for $\sigma > 1$. However, *small-world* behaviour was only found for $-1 < \sigma < 0$, as for $0 < \sigma < 1$ it was found that $\ell \sim (\log(N))^\alpha$. Here we have numerically obtained the scaling of $N(r)$ for large size networks (but still finite, $N = 2^{14}$) and we have measured, using a maximum likelihood algorithm, an effective Hausdorff dimension describing the scaling of $N(r)$ for $r \ll d_{max}$, where d_{max} is the maximum distance between a pair of nodes in the network, namely its diameter. To determine the significance of the effective d_H , we have used a Kolmogorov-Smirnov test. This indicates that the power-law scaling is only significant for $\sigma > 1$ for the sizes considered (see Fig. 12). Analysis of $\ell(N)$ (see App. D) indicates that for $\sigma < 1$ a better scaling is provided by $(\log(N))^\alpha$, in agreement with [58], where $\alpha = 1$ (corresponding to *small-world* behavior) cannot be excluded.

In order to clarify the possible *small-world* nature of the K1d networks for $\sigma < 1$, we have analysed the scaling of $\ell(N)$ (see Fig. 13) [55]. Our results confirm that, for $\sigma \geq 1$, the K1d networks have finite d_H , with $\ell \sim N^{1/d_H}$. For $0 < \sigma < 1$, we have found that both a small-world ($\ell(N) \sim \log(N)$) and an intermediate ($\ell(N) \sim \log(N)^\alpha$, $\alpha > 1.0$) are compatible with the data with the sizes considered ($rs > 0.995$, $N = 2^6, 2^7, \dots, 2^{19}$). These results indicate a slow divergence of the Hausdorff dimension for $0 < \sigma < 1$, in agreement with the exact result proven in Ref. [59].

In summary, we have characterised the topological scaling of the model by measuring the Hausdorff dimension of the networks, d_H . As it can be seen, the Hausdorff dimension tends to 1 for large σ , i.e., the network is a one-dimensional chain.

[1] E. A. Guggenheim, J. Chem. Phys. **13**, 253 (1945).
[2] A. Raju, C. B. Clement, L. X. Hayden, J. P. Kent-Dobias, D. B. Liarte, D. Z. Rocklin, and J. P. Sethna, Phys. Rev. X **9**, 021014 (2019).
[3] A. Pelissetto and E. Vicari, Phys. Rep. **368**, 549 (2002).
[4] S. El-Showk, M. Paulos, D. Poland, S. Rychkov, D. Simmons-Duffin, and A. Vichi, Phys. Rev. Lett. **112**, 141601 (2014).
[5] A. Codello and G. D’Odorico, Phys. Rev. Lett. **110**, 141601 (2013).
[6] A. Codello, N. Defenu, and G. D’Odorico, Phys. Rev. D **91**, 105003 (2015).
[7] H. E. Stanley, *Introduction to Phase Transitions and*

Critical Phenomena (Oxford University Press, 1987).
[8] S. Sachdev, *Quantum Phase Transitions* (Cambridge Univ. Press, Cambridge, 1999).
[9] B. B. Machta, S. L. Veatch, and J. P. Sethna, Phys. Rev. Lett. **109**, 138101 (2012).
[10] A. Alexakis and L. Biferale, Phys. Rep. **767**, 1 (2018).
[11] M. Kardar, Phys. Rep. **301**, 85 (1998).
[12] A. Shekhawat, S. Zapperi, and J. P. Sethna, Phys. Rev. Lett. **110**, 185505 (2013).
[13] J. L. Cardy and P. Grassberger, J. Phys. A: Math. Gen. **18**, L267 (1985).
[14] S. Boccaletti, V. Latora, Y. Moreno, M. Chavez, and D.-U. Hwang, Phys. Rep. **424**, 175 (2006).

- [15] S. N. Dorogovtsev, A. V. Goltsev, and J. F. F. Mendes, *Rev. Mod. Phys.* **80**, 1275 (2008).
- [16] R. Rammal, *J. Stat. Phys.* **36**, 547 (1984).
- [17] R. Burioni and D. Cassi, *Phys. Rev. Lett.* **76**, 1091 (1996).
- [18] G. Bianconi and S. N. Dorogovtsev, *J. Stat. Mech.* **2020**, 014005 (2020).
- [19] J. J. Torres and G. Bianconi, arXiv:2001.05934 (2020).
- [20] M. Reitz and G. Bianconi, arXiv:2003.09143 (2020).
- [21] F. Battiston, G. Cencetti, I. Iacopini, V. Latora, M. Lucas, A. Patania, J.-G. Young, and G. Petri, arXiv:2006.01764 (2020).
- [22] R. Albert and A.-L. Barabási, *Rev. Mod. Phys.* **74**, 47 (2002).
- [23] L. K. Gallos, H. A. Makse, and M. Sigman, *Proceedings of the National Academy of Sciences* **109**, 2825 (2012).
- [24] S. Carmi, S. Carter, J. Sun, and D. ben Avraham, *Phys. Rev. Lett.* **102**, 238702 (2009).
- [25] G. Li, S. D. S. Reis, A. A. Moreira, S. Havlin, H. E. Stanley, and J. S. Andrade, *Phys. Rev. Lett.* **104**, 018701 (2010).
- [26] T. Weng, M. Small, J. Zhang, and P. Hui, *Scientific Reports* **5**, 17309 (2015).
- [27] N. Masuda, M. A. Porter, and R. Lambiotte, *Phys. Rep.* **716**, 1 (2017).
- [28] A. Arenas, A. Díaz-Guilera, J. Kurths, Y. Moreno, and C. Zhou, *Phys. Rep.* **469**, 93 (2008).
- [29] G. S. Joyce, *Phys. Rev.* **146**, 349 (1966).
- [30] F. J. Dyson, *Communications in Mathematical Physics* **12**, 91 (1969).
- [31] Y. Meurice, *J. Phys. A: Math. Th.* **40**, R39 (2007).
- [32] M. C. Angelini, G. Parisi, and F. Ricci-Tersenghi, *Phys. Rev. E* **89**, 062120 (2014).
- [33] N. Defenu, A. Trombettoni, and A. Codello, *Phys. Rev. E* **92**, 052113 (2015).
- [34] N. Defenu, A. Trombettoni, and S. Ruffo, *Phys. Rev. B* **96**, 104432 (2017).
- [35] G. Gori, M. Michelangeli, N. Defenu, and A. Trombettoni, *Phys. Rev. E* **96**, 012108 (2017).
- [36] L. Leuzzi and G. Parisi, *Phys. Rev. B* **88**, 224204 (2013).
- [37] M. I. Berganza and L. Leuzzi, *Phys. Rev. B* **88**, 144104 (2013).
- [38] F. Cescatti, M. Ibáñez Berganza, A. Vezzani, and R. Burioni, *Phys. Rev. B* **100**, 054203 (2019).
- [39] R. A. Baños, L. A. Fernandez, V. Martin-Mayor, and A. P. Young, *Phys. Rev. B* **86**, 134416 (2012).
- [40] H. G. Katzgraber, D. Larson, and A. P. Young, *Phys. Rev. Lett.* **102**, 177205 (2009).
- [41] C. Behan, L. Rastelli, S. Rychkov, and B. Zan, *Phys. Rev. Lett.* **118**, 241601 (2017).
- [42] C. Behan, L. Rastelli, S. Rychkov, and B. Zan, *J. Phys. A: Math. Theor.* **50**, 354002 (2017).
- [43] Y. Gefen, B. B. Mandelbrot, and A. Aharony, *Phys. Rev. Lett.* **45**, 855 (1980).
- [44] Y. Gefen, A. Aharony, Y. Shapir, and B. B. Mandelbrot, *J. Phys. A: Math. Gen.* **17**, 435 (1984).
- [45] Y. Gefen, A. Aharony, and B. B. Mandelbrot, *J. Phys. A: Math. Gen.* **17**, 1277 (1984).
- [46] T. Jonsson and J. F. Wheeler, *Nucl. Phys. B* **515**, 549 (1998).
- [47] B. Durhuus, T. Jonsson, and J. F. Wheeler, *J. Stat. Phys.* **128**, 1237 (2007).
- [48] J. Kleinberg, in *Proceedings of the Thirty-Second Annual ACM Symposium on Theory of Computing*, STOC'00 (Association for Computing Machinery, New York, NY, USA, 2000) p. 163170.
- [49] D. J. Watts and S. H. Strogatz, *Nature (London)* **393**, 440 (1998).
- [50] P. Expert, S. de Nigris, T. Takaguchi, and R. Lambiotte, *Phys. Rev. E* **96**, 012312 (2017).
- [51] S. De Nigris and X. Leoncini, *Phys. Rev. E* **91**, 042809 (2015).
- [52] P. Grassberger, *Journal of Statistical Mechanics: Theory and Experiment* **2013**, 04004 (2013).
- [53] P. Grassberger, *Journal of Statistical Physics* **153**, 289 (2013).
- [54] V. Latora and M. Marchiori, *Phys. Rev. Lett.* **87**, 198701 (2001).
- [55] M. E. J. Newman, *Networks: An Introduction* (Oxford University Press, 2011).
- [56] P. Erdős and A. Rényi, *Studia Sci. Math. Hungar* **3**, 459 (1968).
- [57] D. J. Watts and S. H. Strogatz, *Nature* **393**, 440 (1998).
- [58] K. Kosmidis, S. Havlin, and A. Bunde, *EPL (EuroPhys. Lett.)* **82**, 48005 (2008).
- [59] M. Biskup, *Ann. Probab.* **32**, 2938 (2004).
- [60] P. Van Mieghem, *Graph spectra for complex networks* (Cambridge University Press, 2010).
- [61] R. Burioni and D. Cassi, *Modern Phys. Lett. B* **11**, 1095 (1997).
- [62] J. D. Noh and H. Rieger, *Phys. Rev. Lett.* **92**, 118701 (2004).
- [63] A. Clauset, C. R. Shalizi, and M. E. Newman, *SIAM review* **51**, 661 (2009).
- [64] A. Klaus, S. Yu, and D. Plenz, *PloS one* **6**, 1 (2011).
- [65] J. Alstott and D. P. Bullmore, *PloS one* **9**, 1 (2014).
- [66] S. Wu and Z. R. Yang, *J. Phys. A: Math. Gen.* **28**, 6161 (1995).
- [67] K. G. Wilson and J. Kogut, *Phys. Rep.* **12**, 75 (1974).
- [68] E. Brézin and J. Zinn-Justin, *Phys. Rev. Lett.* **36**, 691 (1976).
- [69] E. Brezin and et al., *The Large N Expansion in Quantum Field Theory and Statistical Physics* (World Scientific Publishing, 1993).
- [70] M. Moshe and J. Zinn-Justin, *Phys. Rep.* **385**, 69 (2003).
- [71] E. Efrati, Z. Wang, A. Kolan, and L. P. Kadanoff, *Rev. Mod. Phys.* **86**, 647 (2014).
- [72] H. Kleinert and V. Schulte-Frohlinde, *Critical Properties of ϕ^4 -Theories* (World Scientific Publishing, 2001).
- [73] J. Zinn-Justin, *Quantum field theory and critical phenomena; 3rd ed.*, International series of monographs on physics (Clarendon Press, Oxford, 1996).
- [74] J. Polchinski, *Nucl. Phys. B* **231**, 269 (1984).
- [75] F. J. Wegner and A. Houghton, *Phys. Rev. A* **8**, 401 (1973).
- [76] C. Wetterich, *Phys. Lett. B* **301**, 90 (1993).
- [77] N. Defenu and A. Codello, *Phys. Rev. D* **98**, 016013 (2018).
- [78] N. Defenu, P. Mati, I. G. Márián, I. Nándori, and A. Trombettoni, *J. High Energy Phys.* **2015**, 141 (2015).
- [79] S. Yabunaka and B. Delamotte, *Phys. Rev. Lett.* **119**, 191602 (2017).
- [80] S. Yabunaka and B. Delamotte, *Phys. Rev. Lett.* **121**, 231601 (2018).
- [81] N. Defenu and A. Codello, arXiv e-prints, arXiv:2005.10827 (2020), arXiv:2005.10827 [cond-mat.stat-mech].

- [82] J. L. Cardy and H. W. Hamber, Phys. Rev. Lett. **45**, 499 (1980).
- [83] R. Peled and Y. Spinka, arXiv:1708.00058 (2017).
- [84] H. E. Stanley, Phys. Rev. Lett. **20**, 589 (1968).
- [85] P. G. de Gennes, Phys. Lett. A **38**, 339 (1972).
- [86] R. Balian and G. Toulouse, Phys. Rev. Lett. **30**, 544 (1973).
- [87] M. E. Fisher, Phys. Rev. Lett. **30**, 679 (1973).
- [88] S. El-Showk, M. F. Paulos, D. Poland, S. Rychkov, D. Simmons-Duffin, and A. Vichi, Phys. Rev. D **86**, 025022 (2012).
- [89] Y. Holovatch, Theoretical and Mathematical Physics **96**, 1099 (1993).
- [90] S. El-Showk, M. F. Paulos, D. Poland, S. Rychkov, D. Simmons-Duffin, and A. Vichi, Phys. Rev. D **86**, 025022 (2012).
- [91] A. Cappelli, L. Maffi, and S. Okuda, Journal of High Energy Physics **2019**, 161 (2019).
- [92] D. Cassi, Phys. Rev. Lett. **68**, 3631 (1992).
- [93] R. Burioni, D. Cassi, and A. Vezzani, Phys. Rev. E **60**, 1500 (1999).
- [94] D. Cassi, Phys. Rev. Lett. **76**, 2941 (1996).
- [95] R. Burioni, D. Cassi, and A. Vezzani, J. Phys. A: Math. Theor. **32**, 5539 (1999).
- [96] S. Bradde, F. Caccioli, L. Dall'Asta, and G. Bianconi, Phys. Rev. Lett. **104**, 218701 (2010).
- [97] K. Hattori, T. Hattori, and H. Watanabe, Progress of Theoretical Physics Supplement **92**, 108 (1987).
- [98] D. Cassi and L. Fabbian, J. Phys. A: Math. Gen. **32**, L93 (1999).
- [99] R. Burioni, D. Cassi, and C. Destri, Phys. Rev. Lett. **85**, 1496 (2000).
- [100] P. F. Buonsante, R. Burioni, D. Cassi, I. Meccoli, S. Regina, and A. Vezzani, Physica A **280**, 131 (2000).
- [101] A. Maritan and A. Stella, Phys. Rev. B **34**, 456 (1986).
- [102] R. Thouy, R. Jullien, and C. Benoit, Journal of Physics Condensed Matter **7**, 9703 (1995).
- [103] U. R. Freiberg, "Some remarks on the Hausdorff and spectral dimension of v-variable nested fractals," in *Recent Developments in Fractals and Related Fields*, edited by J. Barral and S. Seuret (Birkhäuser Boston, Boston, 2010) pp. 267–282.
- [104] J. K. Rudra and J. J. Kozak, Phys. Lett. A **151**, 429 (1990).
- [105] R. Burioni and D. Cassi, Phys. Rev. E **49**, R1785 (1994).
- [106] A. Alexander and R. Orbach, J. Phys. (Paris) Lett. **43**, L625 (1982).
- [107] D. C. Hong, S. Havlin, H. J. Herrmann, and H. E. Stanley, Phys. Rev. B **30**, 4083 (1984).
- [108] E. Bullmore and O. Sporns, Nature Reviews Neuroscience **10**, 186 (2009).
- [109] L. Papadopoulos, M. A. Porter, K. E. Daniels, and D. S. Bassett, Journal of Complex Networks **6**, 485 (2018).
- [110] R. Pastor-Satorras, C. Castellano, P. Van Mieghem, and A. Vespignani, Rev. Mod. Phys. **87**, 925 (2015).
- [111] S. N. Dorogovtsev, A. V. Goltsev, and J. F. F. Mendes, Rev. Mod. Phys. **80**, 1275 (2008).
- [112] A. L. Barabási and R. Albert, Science **286**, 509 (1999).
- [113] E. Farhi, J. Goldstone, S. Gutmann, J. Lapan, A. Lundgren, and D. Preda, Science **292**, 472 (2001).
- [114] S. van Frank, M. Bonneau, J. Schmiedmayer, S. Hild, C. Gross, M. Cheneau, I. Bloch, T. Pichler, A. Negretti, T. Calarco, and S. Montangero, Scientific Reports **6**, 34187 (2016).
- [115] P. Doria, T. Calarco, and S. Montangero, Phys. Rev. Lett. **106**, 190501 (2011).
- [116] M. Born and V. Fock, Zeitschrift für Physik **51**, 165 (1928).
- [117] W. H. Zurek, U. Dorner, and P. Zoller, Phys. Rev. Lett. **95**, 1301 (2005).
- [118] R. Barankov and A. Polkovnikov, Phys. Rev. Lett. **101**, 076801 (2008).
- [119] G. Bigan Mbeng, R. Fazio, and G. Santoro, arXiv:1906.08948 (2019).
- [120] N. Defenu, T. Enss, M. Kastner, and G. Morigi, Phys. Rev. Lett. **121**, 240403 (2018).
- [121] N. Defenu, G. Morigi, L. Dell'Anna, and T. Enss, Phys. Rev. B **100**, 184306 (2019).
- [122] C. Monroe, W. C. Campbell, L. M. Duan, Z. X. Gong, A. V. Gorshkov, P. Hess, R. Islam, K. Kim, G. Pagano, P. Richerme, C. Senko, and N. Y. Yao, arXiv e-prints, arXiv:1912.07845 (2019).
- [123] A. Keesling, A. Omran, H. Levine, H. Bernien, H. Pichler, S. Choi, R. Samajdar, S. Schwartz, P. Silvi, S. Sachdev, P. Zoller, M. Endres, M. Greiner, Vuletić, V., and M. D. Lukin, Nature **568**, 207 (2019).
- [124] D. Mulder and G. Bianconi, J. Stat. Phys. **173**, 783 (2018).
- [125] M. Boguna, I. Bonamassa, M. De Domenico, S. Havlin, D. Krioukov, and M. Serrano, arXiv:2001.03241 (2020).
- [126] Z. Wu, G. Menichetti, C. Rahmede, and G. Bianconi, Scientific Reports **5**, 1 (2015).
- [127] G. Bianconi and C. Rahmede, Phys. Rev. E **93**, 032315 (2016).
- [128] A. P. Millán, J. J. Torres, and G. Bianconi, Phys. Rev. E **99**, 022307 (2019).
- [129] A. P. Millán, J. J. Torres, and G. Bianconi, arXiv:1912.04405 (2019).
- [130] R. Burioni, D. Cassi, and L. Donetti, J. Phys. A: Math. Gen. **32**, 5017 (1999).
- [131] D. C. Hong, S. Havlin, H. J. Herrmann, and H. E. Stanley, Phys. Rev. B **30**, 4083 (1984).
- [132] G. Kozma and A. Nachmias, Inventiones Mathematicae **178**, 635 (2009).